ACS APPLIED MATERIALS & INTERFACES

RESEARCH ARTICLE

www.acsami.org

# Fabrication of Vertically Aligned Diamond Whiskers from Highly Boron-Doped Diamond by Oxygen Plasma Etching

Chiaki Terashima,*[,†] Kazuki Arihara,[‡] Sohei Okazaki,[‡] Tetsuya Shichi,[‡] Donald A. Tryk,[§] Tatsuru Shirafuji,[⊥] Nagahiro Saito,[†,⊥,#] Osamu Takai,[†,⊥,#] and Akira Fujishima[‡,∥]

[†]Research Center for Materials Backcasting Technology, Graduate School of Engineering, and [⊥]Department of Materials, Physics and Energy Engineering, Graduate School of Engineering, and [#]EcoTopia Science Institute, Nagoya University, Furo-cho, Chikusa-ku, Nagoya 464-8603, Japan

[‡]Technology Research and Development Department, General Technology Division, Central Japan Railway, 1545-33 Ohyama, Komaki City, Aichi 485-0801, Japan

[§]Fuel Cell Nanomaterials Center, University of Yamanashi, 4-3-11 Takeda, Kofu, Yamanashi 400-8511, Japan

[∥]Tokyo University of Science, 1-3 Kagurazaka, Shinjyuku-ku, Tokyo 162-8601, Japan

Supporting Information

**ABSTRACT:** Conductive diamond whiskers were fabricated by maskless oxygen plasma etching on highly boron-doped diamond substrates. The effects of the etching conditions and the boron concentration in diamond on the whisker morphology and overall substrate coverage were investigated. High boron-doping levels (greater than $8.4 \times 10^{20}$ cm$^{-3}$) are crucial for the formation of the nanosized, densely packed whiskers with diameter of ca. 20 nm, length of ca. 200 nm, and density of ca. $3.8 \times 10^{10}$ cm$^{-2}$ under optimal oxygen plasma etching conditions (10 min at a chamber pressure of 20 Pa). Confocal Raman mapping and scanning electron microscopy illustrate that the boron distribution in the diamond surface region is consistent with the distribution of whisker sites. The boron dopant atoms in the diamond appear to lead to the initial fine column formation. This simple method could provide a facile, cost-effective means for the preparation of conductive nanostructured diamond materials for electrochemical applications as well as electron emission devices.

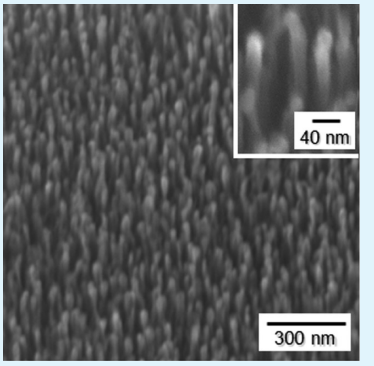


**KEYWORDS:** boron-doped diamond, whisker, nanograss array, reactive ion etching, oxygen plasma, nanostructure

## 1. INTRODUCTION

Carbon-based nanoscale materials such as carbon nanotubes and carbon nanofibers have received a great deal of attention because of the superior properties induced by their unique nanostructures.[1,2] Fabrication of specific types of nanostructures on diamond surfaces is therefore extremely desirable for the improvement of the intrinsic properties of diamond, for example, in field-emission devices because of its negative electron affinity.[3] Nanostructures of conductive diamonds are also of practical importance for such electrochemical applications as biosensors and electrolysis, because the relatively large surface area of such materials may also be an attractive feature when they are used as catalyst supports and substrates for electrochemical reactions. Various functional molecules such as proteins,[4] DNA,[5] and vinylferrocene,[6] as well as metal particles,[7] have been successfully used to modify nanocrystalline, polycrystalline, and single-crystal diamond. The enlargement of the substrate surface area based on the nanostructure, for example, a needlelike structure, with its small diameter, high density, and high aspect ratio, is of great interest for increased reaction efficiency. The development of robust electron emission devices as an alternative to carbon nanotubes in specialized applications could also be highly attractive.

The template synthesis of diamond inside highly ordered porous alumina has already been achieved, resulting in the deposition of well-aligned diamond nanocylinders.[8] As the cylinder size depends on the diameter of the pores in the alumina template, the maximum density of the diamond cylinders has remained at $4.6 \times 10^8$ cm$^{-2}$. The transformation of carbon nanotubes to nanocrystalline diamond has been carried out in a hydrogen plasma at a temperature of 1000 K for 10 h,[9] but the adhesion to the substrate has remained problematic. Other attempts at the anisotropic etching of diamond have been reported in which the surface was covered with nanometer-scale Al and Mo particles as masks for the oxygen plasma.[10,11] In this case, the metal particles deposited were a few nanometers in diameter, and the density of the diamond whiskers formed was $3.0 \times 10^9$ cm$^{-2}$. For higher density, it appears to be necessary to construct a mask at the atomic level. In recent years, the AIST (Japan) and IAF (Germany) groups have developed the fabrication of vertically aligned nanowires by the use of nanodiamond particles as a hard mask for reactive ion etching

**Received:** August 21, 2010
**Accepted:** December 7, 2010
**Published:** January 7, 2011





dx.doi.org/10.1021/am1007722 | *ACS Appl. Mater. Interfaces* 2011, 3, 177–182

(RIE).[12−14] However, these methods are unfavorable for large-scale fabrication and are complicated, because an etching mask needs be intentionally deposited by prepreparation processes. For practical applications, the method used for diamond nanostructures with high density should be simple, low-cost, and reproducible.

More recently, our group and others have reported the electrochemical application of boron-doped diamond nanograss arrays or nanowires prepared via simple techniques on the diamond surface.[15−17] The details of the process conditions, which involve maskless RIE with an oxygen plasma, have heretofore not been described. It is of considerable interest to study the RIE conditions along with the known characteristics of the diamond films to both improve the reproducibility, and to elucidate the etching mechanism, thus facilitating the further development of nanomaterial construction techniques. In this paper, we report the formation of vertically aligned diamond whiskers with a density of approximately $3.8 \times 10^{10}$ $cm^{-2}$ on highly boron-doped diamond thin films by RIE. The relationship of the etching conditions and the diamond characteristics that affect the RIE are also presented, particularly as they relate to the whisker morphologies. The procedure is very simple: it is not necessary to predeposit metal or diamond particles or to apply a photolithographic process but simply to treat the highly boron-doped diamond surface with an oxygen plasma. The feature of this technique that is most scientifically interesting is that dopant atoms in the diamond appear to lead to the initial fine column formation, and the high dopant concentration contributes to the nanosized, densely packed, yet well dispersed, diamond whiskers.

## 2. EXPERIMENTAL SECTION

Polycrystalline boron-doped diamond thin films were grown on Si(111) substrates using a 2.45 GHz microwave plasma chemical vapor deposition (CVD) system equipped with an 8 kW microwave plasma CVD reactor (Seki Technotron Corp., Model AX6500). A mixture of acetone and methanol in the ratio of 9/1 (v/v) was used as the carbon source. $B_2O_3$ as the boron source was dissolved in the acetone-methanol solution at the desired concentrations. The acetone-methanol-$B_2O_3$ solution was sparged with high-purity hydrogen gas. For example, when the boron to carbon (B/C) weight ratio in the solution was 10 000 ppm, the boron doping level in the diamond film estimated by secondary ion mass spectroscopic (SIMS) measurements was $2.1 \times 10^{21}$ $cm^{-3}$. The etching experiments were performed in a parallel plate RIE plasma system with an RF power of 13.56 MHz (SAMCO, RIE-10NR) using an oxygen-based plasma. The diamond thin film specimen on a Si substrate was placed on a quartz holder, which was situated on the self-biased electrode in the RIE chamber. The amounts of boron atoms in the diamond films were evaluated using a CAMECA IMS-6f instrument. As a primary ion, $O_2^+$ accelerated at 5.5 kV was used. The samples were studied by field-emission scanning electron microscopy (FESEM) (Hitachi, S-4800) with a 20 kV accelerating voltage, and characterized by micro-Raman spectroscopy using a Renishaw in-Via Reflex instrument with the 514.5 nm line of an $Ar^+$ laser as the excitation source. All Raman spectra were represented as the average of ten measurement points. X-ray diffraction (XRD) studies were made with a PANalytical X'Pert-PRO MPD with a Cu target. Atomic force microscopy (AFM) (JEOL, JSPM-5200) was used to evaluate the surface morphology characterization of as-deposited, mirror-polished and etched diamond films. The AFM images were captured in tapping mode by use of a silicon cantilever. The mirror-polishing of the diamond was carried out by Namiki Precision Jewel Co. (Tokyo, Japan), by a proprietary technique in which the as-deposited polycrystalline diamond surface was mechanically polished.

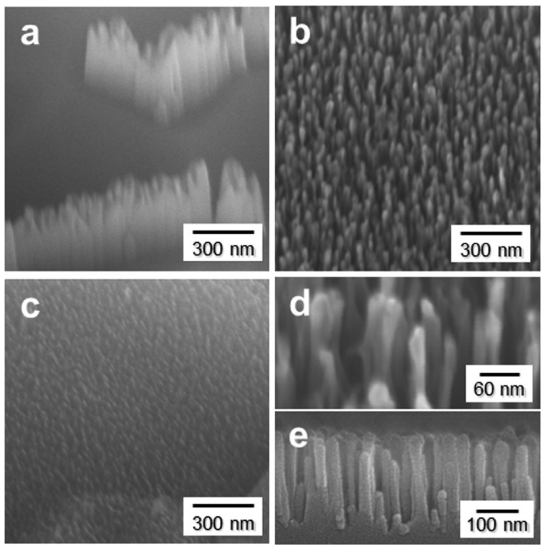


**Figure 1.** SEM images of diamond surfaces ($n_B = 2.1 \times 10^{21}$ $cm^{-3}$) treated with an oxygen plasma for 10 min under (a) $O_2$ gas pressure 5 Pa, (b) 20 Pa, and (c) 100 Pa. The images were collected at tilt angle of 30°. (d) Enlarged and (e) cross-sectional images of b. Only image e was sputtered with platinum to minimize charging of the sample.

## 3. RESULTS AND DISCUSSION

**3.1. Requirement of the Whisker Formation. 3.1.1. Examination of the RIE Conditions.** FESEM was used to investigate the effect of various preparation conditions on the diamond whisker morphology and overall substrate coverage. Figure 1 shows the etched diamond surfaces (boron number density $n_B$ of $2.1 \times 10^{21}$ $cm^{-3}$) under different $O_2$ gas pressures. The gas flow rate was 10 sccm, except for the case of 100 Pa, in which 30 sccm was necessary to control the relatively high pressure. The RF power and the etching duration were 300 W and 10 min, respectively. As shown in Figure 1a, etching at a low pressure of 5 Pa resulted in the production of diamond whiskers of a few hundred nanometers in diameter in a network-like pattern along grain boundaries with poor uniformity. Figure 1b gives the result of the highly dense, yet well-separated vertically aligned diamond whiskers obtained when the RIE was performed at a pressure of 20 Pa. As can be seen from the enlarged and cross-sectional SEM images d and e in Figure 1, the whiskers were distributed uniformly over the surface, and the density was as high as $3.8 \times 10^{10}$ $cm^{-2}$ estimated by the diameter of approximately 20 nm and the distance between each whisker of around 50 nm; the length was approximately 200 nm. At the higher pressure of 100 Pa, fine columns of a few nanometers in size were formed on the overall surface including facets and grain boundaries (Figure 1c). In the case of the higher pressures, the plasma ion densities were relatively high, so that the average kinetic energies of the oxygen atoms were reduced because of inelastic collisions with each other. As a result, fine columns were uniformly fabricated on the diamond surface due to the lower energy, high density plasmas. On the other hand, when the pressure was reduced to 5 Pa, the relatively large nonuniform whiskers may result from the low density plasmas with higher average kinetic energy. The possible reason why the whiskers are formed along grain boundaries at a low pressure will be discussed in a later section. To obtain the effective formation of diamond whiskers with high density and high aspect ratio, therefore, we found that the optimal RIE condition

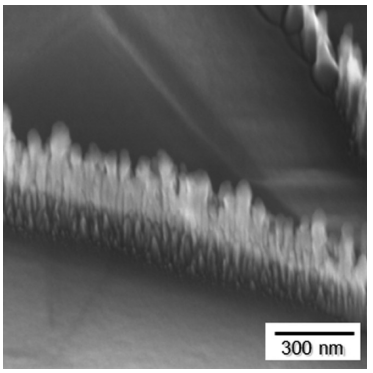


**Figure 2.** SEM images of lightly boron-doped diamond ($n_B$ = 4.3 × $10^{19}$ $cm^{-3}$) etched at a pressure of 20 Pa, $O_2$ gas flow rate of 10 sccm, RF power of 300 W, and etching duration of 10 min.

was as follows: a pressure of 20 Pa, $O_2$ gas flow rate of 10 sccm, RF power of 300 W and an etching duration of 10 min. Under these conditions, if only the RF power was lowered to 70 W, there were no whiskers with high aspect ratio but just fine columns on the diamond surface. It is highly likely that the formation of high density uniform diamond whisker arrays can only be achieved with high ion kinetic energies and plasma ion densities, which are obtained at a pressure of 20 Pa and a high RF power. The doping level of boron in the diamond is also a very critical factor (see below).

**3.1.2. Dependence of Boron Concentration on the Whisker Formation.** The following RIE experiments were then carried out under the previously defined optimal conditions. To examine the effect of boron concentration on the whisker formation, lightly boron-doped diamond with a doping level $n_B$ of 4.3 × $10^{19}$ $cm^{-3}$ was etched under similar conditions. As shown in Figure 2, the formation sites were limited to areas along the grain boundaries, resulting in fringe-like structures. Baik et al. and Li et al. also observed the similar SEM images from nondoped as-deposited diamond film etching in $O_2$ RF plasma.[10,18] They reported the reason why the fringelike structures were probably a consequence of the presence of $sp^2$ carbon at the grain boundaries. It is likely that the easily etched carbon atoms, which are considerably being present at grain boundaries, are redeposited resulting in the relatively higher fibrous structures. In contrast, the result of highly boron-doped diamond ($n_B$ = 2.1 × $10^{21}$ $cm^{-3}$) shown in Figure 1b illustrated that the vertically aligned diamond whiskers were uniformly formed. Note that the etching conditions were the same, except for the amount of boron doped in the diamond films. With an increase of boron concentration, the formation sites extended from the grain boundaries to the facets (data not shown). The whisker density appears to plateau at around 4 × $10^{10}$ $cm^{-2}$ at $n_B \geq 8.4 \times 10^{20}$ $cm^{-3}$. It is worth noting that diamond whiskers have often been formed unintentionally, in an uncontrolled fashion, on diamond substrates.[10,11,19] Zhang et al. also reported the fabrication of nanodiamond cones and whiskers on nanodiamond film surfaces by maskless RIE process.[20−22] The decreased cone density and the size nonuniformity depended on the formation mechanism that the conical/whisker structures were involved with the original column structure of nanodiamond films. In our case, highly dense, homogeneous fine, aligned nanosized diamond whiskers have been successfully prepared without predeposition of metal or diamond particle masks as well as nanodiamond subcolumn.

**3.2. Formation Mechanism of Diamond Whiskers. 3.2.1. Effects of Adventitious Impurities As an Etching Mask.** To study

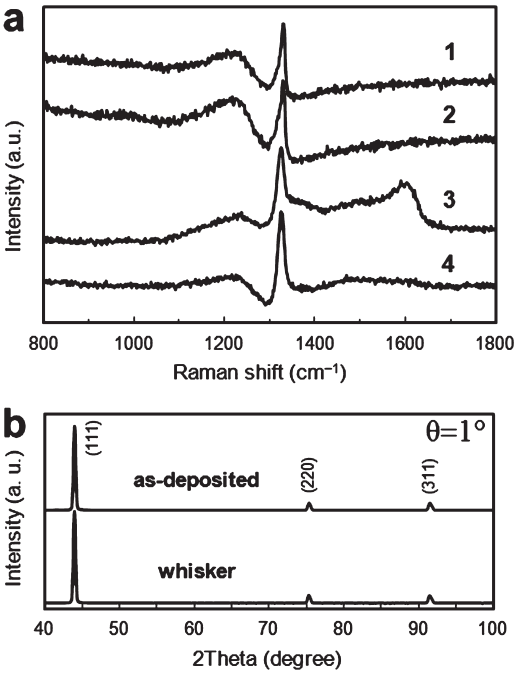


**Figure 3.** Micro-Raman spectra and XRD patterns in the vicinity of the highly boron-doped diamond surface before and after oxygen plasma etching. (a) Raman spectra of (1, 2) growth surfaces and (3, 4) nucleation surfaces, where (1, 3) designate before and (2, 4) after oxygen plasma treatment. (b) Glancing-angle XRD diffraction measurements were performed at an angle $\theta$ of 1°.

the characteristics of the vertically aligned diamond whiskers formed by the oxygen plasma etching of diamond with $n_B$ = 2.1 × $10^{21}$ $cm^{-3}$ and to gain deeper insight into their formation mechanism, FESEM/energy-dispersive X-ray spectroscopy (EDXS), micro-Raman spectroscopy, and XRD were used. One of the known formation mechanisms involves the presence of adventitious impurities, e.g., metal nanoparticles sputtered from a sample holder can act as a mask.[10] In the present work, EDXS indicated only a trace of silicon impurity (0.05 at %), due to sputtering of the quartz holder. Although it could be possible that there was a micromask effect due to the presence of impurities, because silicon, metal, and their oxides are known to be etching masks for diamond, the present case does not appear to involve this mechanism. The fibrous structures observed on lightly boron-doped diamond were formed only along the grain boundaries, even though the silicon impurity was detected at the same level on both lightly and highly boron-doped diamond.

**3.2.2. Effects of the Electrical Characteristics.** It is significant that boron was crucial for the whisker formation. To determine whether the electrical characteristics imparted by boron were involved, we examined the influence of the specimen conductivity on the whisker formation. Kobashi et al. previously reported that the diamond specimen must be electrically conductive for the formation of fibrous structures by hydrogen plasma treatment for 3−6 h under DC bias.[23] The Mo specimen holder was negatively biased, and the substrate for diamond films was required to be conductive. In our experiment, however, the specimen conductivity may not be playing an important role for the whisker formation, because the quartz holder for the RIE was nonconductive. Also, the etching of the highly boron-doped diamond thin film, even though the thickness was below 1 $\mu$m, on nonconductive silicon or diamond substrates resulted in the formation of diamond whiskers. Moreover, when electrically

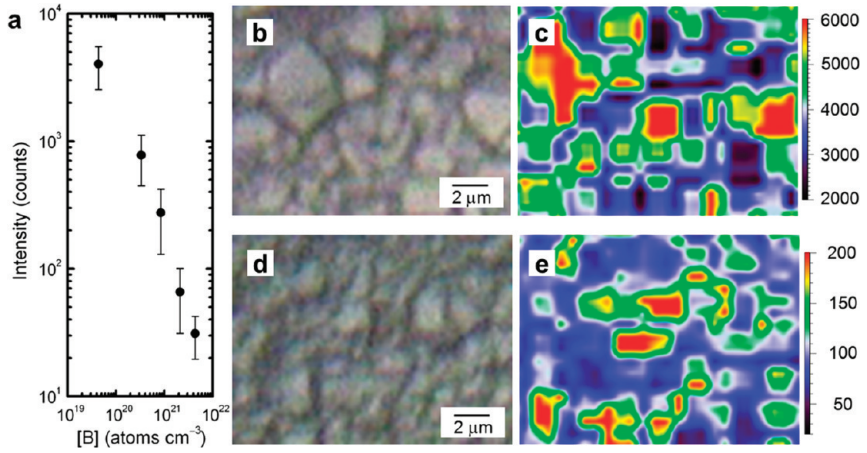


**Figure 4.** Confocal Raman mapping of the diamond line intensity showing the boron distribution. (a) Plot of the diamond (1329 cm$^{-1}$) Raman intensity vs boron concentration in the diamond film. (b) Optical image of the lightly boron-doped diamond ($n_B = 4.3 \times 10^{19}$ cm$^{-3}$). (c) Raman mapping of the same region as (b). (d) Optical image of highly boron-doped diamond ($n_B = 2.1 \times 10^{21}$ cm$^{-3}$). (e) Raman mapping of the same region as (d).

conductive glassy carbon was treated with the oxygen plasma, its surface did not show whisker formation but merely became roughened.

**3.2.3. Effects of the Defects Incorporated in Diamond.** As another possibility, defects incorporated in the diamond during growth in the presence of boron were also speculated to contribute to the selective formation of diamond whiskers, due to the presence of C−C bond strain. Therefore, the vicinity of the diamond surface was examined in more detail, with micro-Raman spectroscopy with a depth resolution of approximately 1.5 $\mu$m and glancing-angle (1°) XRD. These were performed on as-deposited highly boron-doped diamond and vertically aligned diamond whiskers after oxygen plasma etching (Figure 3). The Raman spectrum for the nucleation side of as-deposited diamond (curve 3, Figure 3a), from which the Si substrate had been removed by etching in HF-$HNO_3$ solution, indicated the presence of amorphous nondiamond $sp^2$ carbon, evidenced by the broad band in the 1500 − 1600 cm$^{-1}$ region, which disappeared after oxygen plasma etching (curve 4, Figure 3a). Thus, the present method of RIE enables us to selectively remove the $sp^2$ carbon, without greatly affecting the characteristic, sharp diamond phonon peak at 1329 cm$^{-1}$ or the broader peak 1230 cm$^{-1}$, which is associated with heavy boron doping.[24] In fact, if boron-associated defects were selectively etched, we would have expected the latter peak to decrease in intensity. Thus, the Raman spectra (curves 1 and 2 in Figure 3a) and XRD spectra suggest that the film quality was not affected by the etching process.

**3.2.4. Relationship between the Boron Distribution and the Whisker Sites.** A confocal Raman mapping study was also carried out to examine in more detail the dependence of the whisker sites on the boron concentration and the boron distribution in the diamond surface region. An inverse relationship between the diamond line intensity and the boron concentration in the diamond film was observed (Figure 4a).[24] Also, optical images (Figure 4b, d) and confocal Raman images (Figures 4c, e), based on the diamond line (1329 cm$^{-1}$) intensity were obtained for the different boron-doped diamonds ($n_B = 4.3 \times 10^{19}$ cm$^{-3}$ for images b and c in Figure 4, and $n_B = 2.1 \times 10^{21}$ cm$^{-3}$ for images d and e in Figure 4). The unique Raman spectral features of boron-doped diamond specimens allow tracking of the boron distribution over the entire diamond surface. The distribution of boron in the diamond surface region expanded from the grain boundaries to the facet areas as the boron concentration increased. This tendency was consistent with the distribution of diamond whisker formation sites. Even though a significant heterogeneity of the boron concentration was observed in the Raman mapping of highly boron-doped diamond (Figure 4e), it was sufficient to produce dense whiskers because of a minimum level being present (for example, $n_B > 9 \times 10^{20}$ cm$^{-3}$ in the lower part of Figure 4e).

**3.2.5. Possible Formation Mechanism.** It is certain that the most important factor in the formation mechanism for the diamond whiskers is the presence of the boron dopant atoms. Some reports have suggested that the surface morphology of as-deposited diamond film has played a key role for the initiation of cone formation.[25,26] In other words, the formation process of diamond cones was interpreted in such a way that the plasma etching was stronger at the side of a hillock than at the top, because of the higher ion-sputtering yield at an oblique incident angle. However, this cone formation process, particularly in the initial stage, is different from that in our experiments, in which we used polycrystalline diamond with a grain size of a few $\mu$m and observed diamond whiskers even on the smooth diamond facets. On the basis of the considerations discussed thus far, we believe that the primary fine columns are due to the more intense electron emission from the boron sites in diamond. Boron-doped diamond is known to enhance the electron emission compared to insulating diamond.[27] The resulting local electrical field around the vicinity of the boron site on the diamond surface appears to contribute to the fine column formation during the oxygen plasma etching. Once the columns are formed even on the facets in the case of highly boron-doped diamond, etching would continuously occur in the depression between the fine columns; as a result, the high aspect ratio of diamond whiskers would be developed. The FESEM observation showed that the whisker diameter gradually grew from 5 nm at the etching time of 30 s to 20 nm at 10 min (see the Supporting Information). The increased diameter with etching time would seem to stem from the selective etching of the formed column; of course, there are redeposition of the etched carbon and the influence of the silicon impurities. On the other hand, in the lightly doped case, boron was incorporated along the grain boundaries so that the formation sites of the diamond whiskers were limited to those areas. Here, we should consider again the case in which the plasma ion

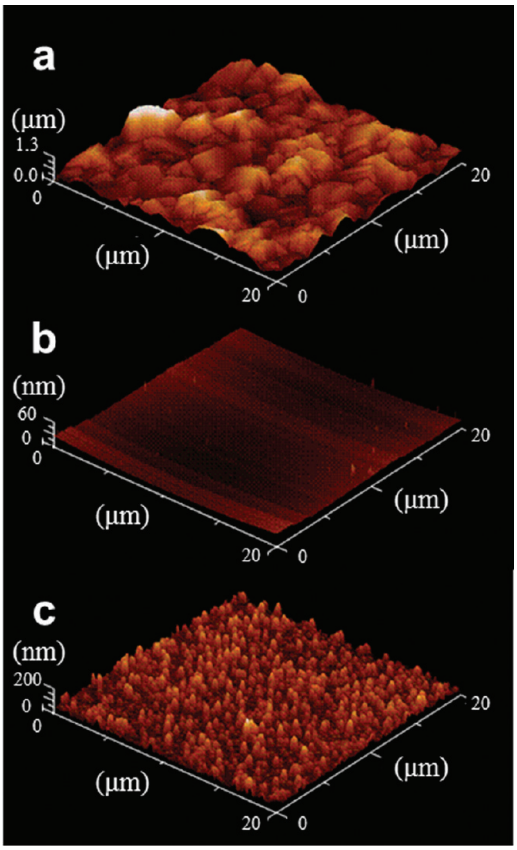


**Figure 5.** Tapping-mode AFM images of (a) as-deposited surface, (b) mechanically polished surface, and (c) resulting diamond surfaces after etching. Field of view: 20 $\mu$m × 20 $\mu$m.

density and ion kinetic energy are relatively low and high, respectively (Figure 1a). In this condition, the low-density plasma with high energy produced at reduced pressures such as 5 Pa might be focused on the grain boundaries. It is very probable in the low-plasma ion density that the enhancement of the electric field will be more favored at diamond grain boundaries, at which it is known that the electrical conductivity can be elevated to levels greater than those on the diamond facets, because of the presence of $sp^2$ carbon, as well as higher boron concentrations, and even to significant concentrations of hydrogen.[28] Consequently, the diamond whiskers of a few hundred nanometers in diameter would be formed in a networklike pattern along the grain boundaries.

**3.3. Fabrication of Large Area Diamond Whisker Covered Surfaces with Coincident Tip Position.** The present fabrication method provides a uniform distribution of diamond whiskers over the whole surface of diamond films in polycrystalline form. We next sought to eliminate the effect of roughness in the polycrystalline diamond films, because the prospect of having a large area of diamond whiskers with the whisker tips in a coincident plane is attractive, both fundamentally, for example, to study the enhancement factor in the field emission experiments, and also technologically, from the applications point of view. Therefore, we examined the etching of mirror-polished boron-doped diamond films. Figure 5 shows AFM images of the as-deposited surface, the polished surface, and the resulting etched diamond surface. The root-mean-square (rms) roughness of the as-deposited diamond was 251 nm, and the mechanical polishing produced a smooth surface with a roughness of 4.1 nm. Upon etching, this smooth surface was converted to the whisker morphology with an rms roughness of 31.4 nm. From the line profile corresponding to Figure 5c (data not shown), the whisker height was estimated as approximately 100 nm, which was half the value measured from the cross-sectional SEM image (Figure 1e). The difference in heights and diameters between the results of the AFM and SEM measurements may have resulted from the size of the cantilever and the medium gain of the AFM. As pointed out in the literature, regarding the AFM-based technique for the measurement of the elastic properties of nanowires aligned on a solid substrate,[29] the disadvantage is its inaccuracy in evaluating the size of the nanowires. The precise AFM measurement of our high-aspect-ratio diamond whiskers was thus difficult. The more important point, however, is that we were able to observe relatively large, flat areas that were uniformly covered with whiskers, with no grain boundaries.

## 4. CONCLUSIONS

Vertically aligned diamond whiskers distributed uniformly on the polycrystalline diamond surface were fabricated from a highly boron-doped diamond thin film by use of oxygen plasma etching. The whisker density and uniformity were significantly dependent on the RIE conditions, especially the chamber pressure, as well as the boron doping level in the diamond. Under the optimal RIE conditions, i.e., oxygen plasma treatment time of 10 min at a pressure of 20 Pa, with an $O_2$ gas flow rate of 10 sccm and plasma power of 300 W, the principal requirement for the whisker formation is a high boron-doping level (greater than $8.4 \times 10^{20}$ $cm^{-3}$). During the initial stages of etching, the boron dopant atoms present at the diamond surface appear to contribute to the extremely small, nanometer-scale structures. It is highly likely that the local enhancement of the electric field near the boron dopant atoms, at which greater numbers of electrons are emitted, will attribute to the preferential etching around the boron sites. This simple technique, utilizing highly boron-doped diamond films which are used as diamond electrodes in electrochemical applications, could provide a facile, cost-effective means for the preparation of nanostructured diamond surfaces for various applications, including those in electrochemistry, for example, in sensors, fuel cells, and electrolytic processes, as well as applications involving robust electron emission devices.

## ■ ASSOCIATED CONTENT

**Ⓢ Supporting Information.** Raman spectra of boron-doped diamond with various boron concentrations, and SEM images obtained after various etching times (PDF). This material is available free of charge via the Internet at http://pubs.acs.org.

## ■ AUTHOR INFORMATION

**Corresponding Author**

*Tel: +81-52-789-5163. Fax: +81-52-789-5163. E-mail: terashima@eco-t.esi.nagoya-u.ac.jp.

## ■ ACKNOWLEDGMENT

This research was conducted at the Central Japan Railway Technology Research and Development Laboratory. C.T. thanks Dr. M. Seki and T. Komine for their encouragement and guidance throughout this research.

## REFERENCES


(1) Hata, K.; Futaba, D. N.; Mizuno, K.; Namai, T.; Yumura, M.; Iijima, S. *Science* **2004**, *306*, 1362–1364.
(2) Boskovic, B. O.; Stolojan, V.; Khan, R. A.; Haq, S.; Silva, S. R. P. *Nat. Mater.* **2004**, *1*, 165–168.
(3) Geis, M. W.; Twichell, J. C.; Lyszczarz, T. M. *J. Vac. Sci. Technol., B* **1996**, *14*, 2060–2067.
(4) Härtl, A.; Schmich, E.; Garrido, J.; Hernando, J.; Catharino, S. C. R.; Walter, S.; Feulner, P.; Kromka, A.; Steinmüller, D.; Stutzmann, M. *Nat. Mater.* **2004**, *3*, 736–742.
(5) Knickerbocker, T.; Strother, T.; Schwartz, M. P.; Russell, J. N., Jr; Butler, J.; Smith, L. M.; Hamers, R. J. *Langmuir* **2003**, *19*, 1938–1942.
(6) Kondo, T.; Hoshi, H.; Honda, K.; Einaga, Y.; Fujishima, A.; Kawai, T. *J. Phys. Chem. C* **2008**, *112*, 11887–11892.
(7) Bennett, J. A.; Show, Y.; Wang, S.; Swain, G. M. *J. Electrochem. Soc.* **2005**, *152*, E184–E192.
(8) Masuda, H.; Yanagishita, T.; Yasui, K.; Nishio, K.; Yagi, I.; Rao, T. N.; Fujishima, A. *Adv. Mater.* **2001**, *13*, 247–249.
(9) Sun, L. T.; Gong, J. L.; Zhu, Z. Y.; Zhu, D. Z.; He, S. X.; Wang, Z. X.; Chen, Y.; Hu, G. *Appl. Phys. Lett.* **2004**, *84*, 2901–2903.
(10) Baik, E.-S.; Baik, Y.-J.; Jeon, D. *J. Mater. Res.* **2000**, *15*, 923–926.
(11) Li, C. Y.; Hatta, A. *Diamond Relat. Mater.* **2005**, *14*, 1780–1783.
(12) Yang, N.; Uetsuka, H.; Osawa, E.; Nebel, C. E. *Angew. Chem., Int. Ed.* **2008**, *47*, 5183–5185.
(13) Yang, N.; Uetsuka, H.; Osawa, E.; Nebel, C. E. *Nano Lett.* **2008**, *8*, 3572–3576.
(14) Nebel, C. E.; Yang, N.; Uetsuka, H.; Osawa, E.; Tokuda, N.; Williams, O. *Diamond Relat. Mater.* **2009**, *18*, 910–917.
(15) Wei, M; Terashima, C.; Lv, M.; Fujishima, A.; Gu, Z.-Z. *Chem. Commun.* **2009**, 3624–3626.
(16) Lv, M.; Wei, M.; Rong, F.; Terashima, C.; Fujishima, A.; Gu, Z.-Z. *Electroanalysis* **2010**, *22*, 199–203.
(17) Szunerits, S.; Coffinier, Y.; Galopin, E.; Brenner, J.; Boukherroub, R. *Electrochem. Commun.* **2010**, *12*, 438–441.
(18) Li, C. Y.; Hatta, A. *Diamond Relat. Mater.* **2006**, *15*, 357–360.
(19) Shiomi, H. *Jpn. J. Appl. Phys.* **1997**, *36*, 7745–7748.
(20) Zou, Y. S.; Ma, K. L.; Zhang, W. J.; Ye, Q.; Yao, Z. Q.; Chong, Y. M.; Lee, S. T. *Diamond Relat. Mater.* **2007**, *16*, 1208–1212.
(21) Zhang, W. J.; Wu, Y.; Wong, W. K.; Meng, X. M.; Chan, C. Y.; Bello, I.; Lifshitz, Y.; Lee, S. T. *Appl. Phys. Lett.* **2003**, *83*, 3365–3367.
(22) Zhang, W. J.; Meng, X. M.; Chan, C. Y.; Wu, Y.; Bello, I.; Lee, S. T. *Appl. Phys. Lett.* **2003**, *82*, 2622–2624.
(23) Kobashi, K.; Tachibana, T.; Yokota, Y.; Kawakami, N.; Hayashi, K.; Yamamoto, K.; Koga, Y.; Fujiwara, S.; Gotoh, Y.; Nakahara, H.; Tsuji, H.; Ishikawa, J.; Köck, F. A.; Nemanich, R. J. *J. Mater. Res.* **2003**, *18*, 305–326.
(24) Prawer, S.; Nemanich, R. J. *Philos. Trans. R. Soc. London, Ser. A* **2004**, *362*, 2537–2565.
(25) Wang, Q.; Li, J. J.; Jin, A. Z.; Wang, Z. L.; Xu, P.; Gu, C. Z. *Diamond Relat. Mater.* **2006**, *15*, 866–869.
(26) Wang, Q.; Li, J. J.; Li, Y. L.; Wang, Z. L.; Gu, C. Z.; Cui, Z. *J. Phys. Chem. C* **2007**, *111*, 7058–7062.
(27) Shih, A.; Yater, J.; Pehrsson, P.; Butler, J.; Hor, C.; Abrams, R. *J. Appl. Phys.* **1997**, *82*, 1860–1867.
(28) Kim, Y. D.; Choi, W.; Wakimoto, H.; Usami, U.; Tomokage, H.; Ando, T. *Diamond Relat. Mater.* **2000**, *9*, 1096–1099.
(29) Song, J.; Wang, X.; Riedo, E.; Wang, Z. L. *Nano Lett.* **2005**, *5*, 1954–1958.